A Novel Numerical Method for Accelerating the Computation of the Steady-State in Induction Machines

A. Bermúdez[a,*], D. Gómez[a], M. Piñeiro[b], P. Salgado[a]

[a] *Dpto. de Matemática Aplicada & Instituto de Matemáticas (IMAT) & Instituto Tecnológico de Matemática Industrial (ITMATI), Universidade de Santiago de Compostela, ES-15782 Santiago de Compostela, Spain*
[b] *Dpto. de Matemática Aplicada, Universidade de Santiago de Compostela, ES-15782 Santiago de Compostela, Spain*

Abstract

This paper presents a novel and efficient methodology to reduce the time needed to reach the steady-state in the finite element simulation of induction machines. More precisely, the work focuses on induction motors with squirrel cage rotor, where sources in the stator coil sides are given in terms of periodic currents. Essentially, the procedure consists in computing suitable initial conditions for the currents in the rotor bars, thus allowing to obtain the steady-state fields of the machine by solving a transient magnetic model in just a few revolutions. Firstly, the mathematical model that simulates the behavior of the machine is introduced. Then, an approximation of this model is developed, from which suitable initial currents are derived by computing the solution in the least-square sense to an overdetermined problem with only two unknowns. Finally, the method is applied to a particular induction machine working under different operating conditions. The results show important computational savings to reach the motor steady-state in comparison with assuming zero initial conditions, which validate the efficiency of the procedure.

Keywords: Steady-state solution; Induction motor; Transient magnetic; Nonlinear partial differential equations; Finite element methods; Periodic solution

1. Introduction

This work deals with the finite element approximation of the steady-state behavior of squirrel cage induction machines by using a fast numerical procedure. For this purpose, a numerical method to compute periodic solutions by determining suitable initial currents in the rotor bars is developed, shortening the transient part of the solution considerably, so that the steady-state is reached in a reduced number of cycles.

Numerical simulation is an essential tool in the design and analysis of electric machines, as it avoids building unnecessary prototypes and significantly reduces both cost and time to obtain new configurations. In particular, the numerical simulation of electric machines by using finite element methods generally requires the solution of a nonlinear system of partial differential equations derived from Maxwell's equations, eventually coupled with thermal, mechanical and/or electric circuit equations (see [1] and references therein).

The electromagnetic model of electric machines is often based on describing the active zone of the motor as a 2D distributed nonlinear eddy current or transient magnetic problem. Indeed, in order to reduce electromagnetic losses, the magnetic cores of electric machines are laminated media consisting of a large number of stacked steel sheets, which are orthogonal to the direction of the currents traversing the stator coil sides. Considering the high number of sheets and their small thickness (usually less than one millimeter), solving a three-dimensional model would require to consider homogenization techniques (see [2]) or a very fine mesh, the latter leading to extremely high computational costs. As a consequence, the usual simulation model consists in an electromagnetic problem defined on a cross-section of the machine, while the end regions

*Corresponding author
Email address: alfredo.bermudez@usc.es (A. Bermúdez)

of the stator windings and some other elements (for instance, the squirrel cage end-rings) are modeled by circuit elements; in this way, the distributed 2D model will be coupled with a lumped one (see, for instance, [3]). On the other hand, the interplay between the magnetic fields in stator and rotor gives raise to a force that causes the latter to rotate around the machine axis. Therefore, the result is a transient eddy current or transient magnetic problem defined in a moving geometry with prescribed speed.

Frequently, the resulting mathematical model needs to be provided with initial conditions which are neither known a priori, nor easy to obtain. Notice that, due to the fact that the rotor currents are caused by the rotating field from the stator, "pure" stationary finite element simulations are not possible, because the stationary rotor bar currents are unknown when the simulations start. When unappropriate values are prescribed for these conditions (for instance, when they are simply set to zero), a very long CPU time is needed to reach the steady-state solution. In fact, the computation of the steady currents can take several days although the engineer is only interested in the final attained state, whose computation would need only a few minutes of computer time if appropriate initial conditions were known. Thus, techniques allowing us to compute the steady solution in the shortest possible time are in high demand and, in particular, those based on determining suitable initial conditions. Notice that the steady solution is independent of these initial conditions. They only affect the time required to achieve the steady-state.

In the literature, we can find several approaches to the problem of reducing the computational cost to reach the steady-state in the numerical simulation of induction motors. The worst case scenario would be what is known as *brute-force method*, which consists in starting with zero initial conditions and letting the simulation advance in time until the steady-state is reached. In this case, long time simulations may be needed, even with the performance of modern computers. In recent years, different techniques have been developed to address the problem we are considering. For example, the so-called *Time Periodic Finite Element Methods* (TPFEM) are based on writing the discretized problem in a time-interval in which its solution is periodic, and solving all time steps simultaneously (see [4]). Even though this method avoids the step-by-step simulation, it requires solving nonlinear systems, which involves dealing with very large non-symmetric matrices. Therefore, parallelization techniques, which can be applied in space or time, are almost unavoidable (see [5]). Alternatively, in the *Time Periodic - Explicit Error Correction Methods* (TP-EEC), (see [6]), and the *Time Differential Correction* (TDC), (see [7]), convergence of the transient model is accelerated by incorporating error correction techniques already present in more general iterative methods, along with some properties of TPFEM. Another strategy is based on using a time-decomposition of the solution in terms of sinusoidal basis functions and obtaining a large system of algebraic equations; this technique is known as *harmonic balance method* and has also been applied in [8] to induction machines. Recently, an approach framed in the so-called *parareal* or *parallel-in-time integration* methods has been introduced in [9]. In that work, the authors try to speed up integration in time by splitting the time-domain and solving several time steps in parallel, thus taking advantage of the parallel architecture of modern computers. Finally, we highlight the methodology which consists in prescribing as initial conditions the ones obtained as the solution to a nonlinear eddy current problem in the frequency domain. In such a case, the harmonic approximation is based on the hypothesis that the time variation of the fields can be written in terms of a complex exponential function. Then the nonlinear effects are taken into account by means of an *effective magnetization curve* and the rotor motion by an adjustment in the electric conductivity of the rotor bars (see [10]).

A common obstacle for TPFEM, TP-EEC and TDC methods is choosing a suitable time interval in which the solution is assumed to be periodic. This is due to the fact that the magnetic fields in rotor and stator oscillate at different frequencies, and the common time at which both are periodic (the so-called *effective period*) is generally quite large. However, at the same time, the periodicity condition has to be defined in a small enough time interval for the method to be useful. In TPFEM methods, there are several strategies to deal with this restriction, most of them based on the spatio-temporal symmetries of the problem ([5]). On the other hand, TP-EEC and TDC methods handle it by accelerating the convergence in both domains separately, or even only in one of them ([6]). A definition of a fundamental frequency common to rotor and stator is also needed in the harmonic balance method. In this regard, our methodology has the advantage of making use of the periodicity condition only in the rotor bars, so that the cited limitations do not apply. Moreover, the computational cost of our approach does not depend on the size of this period, and the number

of unknowns is very small in comparison with the previous methods.

As already said, the main objective of this article is to reduce the simulation time, so that the steady regime is reached in the shortest possible time. For this purpose, we develop a methodology that seeks good approximations of the initial currents in the rotor bars of a squirrel cage induction motor, which allows us to avoid the otherwise long transient state in its simulation. The proposed methodology is inspired in the techniques introduced in [11] for a 2D transient magnetic model with sources given in terms of currents and voltage drops. In the present paper, we will extend some of the ideas proposed in that reference to a case including motion of some parts of the domain and conductors in which neither currents nor voltage drops are known. Moreover, initial currents are sought in these conductors, what represents an additional difficulty.

The outline of the paper is the following. In Section 2 we state the problem to be solved, that consists of a transient 2D nonlinear distributed model coupled with a lumped one for the electrical circuit of the squirrel cage. Then, in Section 3, we will rewrite the problem formally as an implicit system of ODE in terms of the current in the rotor bars of the squirrel cage. Section 4 is devoted to the approximation of the initial condition corresponding to a periodic steady solution. For this purpose, we perform twice a time-integration of the reduced problem, neglect some terms and approximate the currents in the rotor bars by their respective main harmonics. Finally, in Section 5 we validate the method with some numerical results that illustrate its performance.

2. Mathematical Modeling

In this section we present a 2D transient magnetic model that describes the electromagnetic behavior of induction machines. As detailed in the introduction, we follow the strategy of studying a bidimensional distributed problem defined on a cross-section of the induction motor, integrating the end-rings of the squirrel cage by means of a lumped model built with circuit equations. In particular, we assume that the magnetic flux lies on the plane of this section and neglect the effects of eddy currents in the z space direction except along the rotor bars, as the ferromagnetic core is laminated in this direction. Thus, the laminated core can be considered as a homogeneous non-conducting medium.

Eddy currents are usually modelled by the low-frequency Maxwell system of equations:

$$\mathbf{curl}\, \boldsymbol{H} = \boldsymbol{J}, \tag{1}$$

$$\frac{\partial \boldsymbol{B}}{\partial t} + \mathbf{curl}\, \boldsymbol{E} = \mathbf{0}, \tag{2}$$

$$\operatorname{div} \boldsymbol{B} = 0, \tag{3}$$

along with Ohm's law in stationary conductors

$$\boldsymbol{J} = \sigma \boldsymbol{E}, \tag{4}$$

and the constitutive magnetic law

$$\boldsymbol{H} = \nu \boldsymbol{B}, \tag{5}$$

where $\boldsymbol{H}$ is the magnetic field, $\boldsymbol{B}$ is the magnetic flux density, $\boldsymbol{E}$ is the electric field, $\boldsymbol{J}$ is the current density (which is null in dielectrics), $\sigma > 0$ is the electric conductivity in conductors and ν is the magnetic reluctivity, which will be specified later.

Let us assume that the current density $\boldsymbol{J}$ has non-null component only in the z spatial direction and that this component does not depend on z, i.e., $\boldsymbol{J} = J_z(x, y, t)\mathbf{e}_z$. We also assume that the geometry and the magnetic field $\boldsymbol{H}$ are invariant along the z spatial direction, and that all materials are magnetically isotropic. In this case, under an appropriate decay of fields at infinity (see [12]), the magnetic field $\boldsymbol{H}$, and then the magnetic induction $\boldsymbol{B}$, have only components on the $xy-$plane and both are independent of z, i.e.,

$$\boldsymbol{H} = H_x(x, y, t)\mathbf{e}_x + H_y(x, y, t)\mathbf{e}_y,$$
$$\boldsymbol{B} = B_x(x, y, t)\mathbf{e}_x + B_y(x, y, t)\mathbf{e}_y.$$

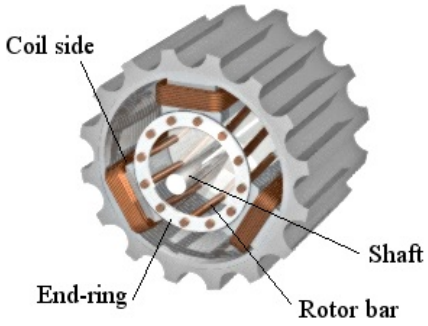

Figure 1: Main parts integrating an induction motor. From Wikimedia Commons by Mtodorov 69 under license CC-BY-SA-3.0.

Since we are interested in using a finite element method for the numerical solution, we will restrict ourselves to a bounded domain. Let us consider the 2D bounded domain Ω, corresponding to the cross-section of the initial configuration of a squirrel cage induction motor (see Figure 1). Hence, domain Ω consists of n_c connected conductors (stator coil sides and rotor bars), the ferromagnetic core (in rotor and stator), the air between rotor and stator (air-gap), and the rotor shaft which will be modeled as air. Moreover, we have considered the outer boundary of the stator as domain boundary, but the same methodology applies with no change to the case in which the motor is surrounded by an artificial box filled with air. In Figure 2 a quarter of domain Ω is shown (the whole domain is sketched in Figure 6). In the sequel, the following notations will be used:

- Ω_0: domain occupied by air (white color in Figure 2).
- Ω_i, $i = 1, \ldots, n_c$: linear conductors representing the cross-sections of the rotor bars ($i = 1, \ldots, n_b$; grey color in Figure 2) and of the stator coil sides ($i = n_b + 1, \ldots, n_c$; blue, yellow and red colors in Figure 2). Furthermore, $\Omega_c := \cup_{i=1}^{n_c} \Omega_i$.
- Ω_{mc}: non-conducting nonlinear magnetic cores (brown color in Figure 2).

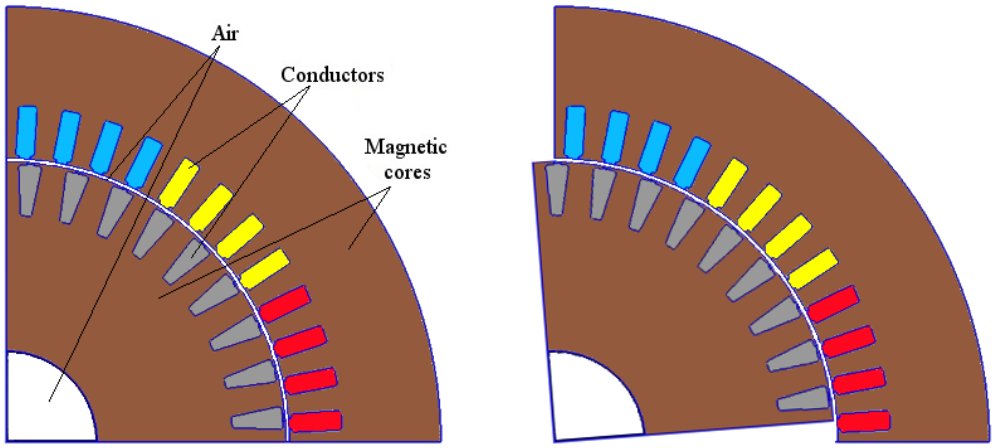

Figure 2: A quarter of domain Ω at time $t = 0$ (left) and $t > 0$ (right). Modification of a picture provided by Robert Bosch GmbH.

Finally, we consider a global magnetic reluctivity function $\nu : \Omega \times [0, \infty) \longrightarrow (0, \infty)$ defined by

$$\nu(x, y; s) := \begin{cases} \nu_0 & \text{if } (x, y) \in \Omega_0, \\ \nu_{\rm c} & \text{if } (x, y) \in \Omega_{\rm c}, \\ \nu_{\rm mc}(s) & \text{if } (x, y) \in \Omega_{\rm mc}, \end{cases}$$

where ν_0 is the reluctivity of the vacuum, $\nu_{\rm c}$ is a constant and $\nu_{\rm mc}(s)$ is a nonlinear function of the magnetic flux, $\nu_{\rm mc}(|\boldsymbol{B}|)$. Notice that the value of $\nu_{\rm c}$ could be different in each conductor Ω_i but we will assume, for the sake of simplicity, that it is the same for all of them.

The eddy current problem (1)–(5) is completed with the boundary condition $\boldsymbol{B} \cdot \boldsymbol{n} = 0$ on $\partial\Omega$, which means there is no magnetic flux through the boundary.

2.1. The Transient Magnetic Model

Now, we are going to obtain the transient magnetic formulation that models the electromagnetic behavior of the induction motor. In particular, we will see how the rotation of the motor can be included in the formulation.

In the method proposed in this paper, we will make a simplification based on assuming that the bars are stranded conductors, that is, conductors where the induced currents are uniformly distributed on their respective cross-sections. In a similar way, we will also treat the stator coil sides as stranded conductors. These assumptions amount to say that the current density field is uniformly distributed in all conducting subdomains Ω_i and is given by

$$J_{z,i}(t) = \begin{cases} \dfrac{y_i(t)}{\text{meas}(\Omega_i)}, & i = 1, \ldots, n_{\rm b}, \\ \dfrac{I_i(t)}{\text{meas}(\Omega_i)}, & i = n_{\rm b} + 1, \ldots, n_{\rm c}, \end{cases}$$

where we have denoted $y_i(t)$, $i = 1, \ldots, n_{\rm b}$, the currents through the cross-section of each rotor bar at time t, and $I_i(t)$, $i = n_{\rm b} + 1, \ldots, n_{\rm c}$, the currents through the cross-section of each stator coil side at time t. We notice that, in the simulation of an induction machine, the bars of the squirrel cage are usually modeled as solid conductors, where, in opposition to stranded conductors, the induced currents are not uniformly distributed (see, for instance, the classical model presented in [3]). Nevertheless, assuming the rotor bars as stranded conductors is not a limitation to the applicability of the method (see Remark 11 in Section 5.2.1).

In order to solve the described two-dimensional model, it is convenient to introduce a magnetic vector potential because it leads to solve a scalar problem instead of a vector one. Since $\boldsymbol{B}$ is divergence-free, there exists a so-called magnetic vector potential $\boldsymbol{A}$ such that $\boldsymbol{B} = \mathbf{curl}\, \boldsymbol{A}$. Under the assumptions above, we can choose a magnetic vector potential that is independent of z and does not have either x or y components, i.e., $\boldsymbol{A} = A_z(x, y, t)\mathbf{e}_z$ (see, for instance, [13]).

We notice that the currents in the rotor bars are not known but we will show how to include in the formulation some additional equations to link currents with potential drops per unit length. However, we advance that these potential drops are not a problem data either, and therefore we will need to couple the PDE problem with a lumped model for the squirrel cage circuit.

For the sake of simplicity, we will assume that the electric conductivity σ is constant for all conductors, but otherwise the development below can be applied with no significant change (see [11]). Taking into account Faraday's law in the rotor bars (2), and the assumptions of invariance under translation in the z-direction and axial direction of currents, we deduce that there exist $n_{\rm b}$ scalar potentials V_i, $i = 1, \ldots, n_{\rm b}$, unique up to a constant, such that

$$\frac{\partial \boldsymbol{A}}{\partial t} + \boldsymbol{E} = -\mathbf{grad}\, V_i \quad \text{in } \Omega_i \times \mathbb{R}, \quad i = 1, \ldots, n_{\rm b}.$$

From the assumptions on $\boldsymbol{J}$ and Ohm's law (4), we deduce that $\boldsymbol{E}$ in the rotor bars has non-null component only in the z spatial direction which is, furthermore, spatially constant in each Ω_i, $i = 1, \ldots, n_{\rm b}$. Moreover,

since $\boldsymbol{A} = A_z(x,y,t)\mathbf{e}_z$, we have

$$-\mathbf{grad}\, V_i = -\frac{\partial V_i}{\partial z}\mathbf{e}_z$$

in each Ω_i, $i = 1,\dots,n_{\rm b}$. As a consequence, the above equation reduces to

$$\frac{\partial A_z}{\partial t} + E_z = -C_i(t) \quad \text{in } \Omega_i, \quad i = 1,\dots,n_{\rm b}, \tag{6}$$

where $C_i(t) := (\partial V_i/\partial z)(t)$ is the potential drop per unit length along direction z in conductor Ω_i, $i = 1,\dots,n_{\rm b}$. Multiplying (6) by the electric conductivity, integrating on each Ω_i, $i = 1,\dots,n_{\rm b}$, and taking Ohm's law into account we deduce

$$\frac{d}{dt}\int_{\Omega_i} \sigma A_z(x,y,t)\,dxdy + y_i(t) = -C_i(t)\sigma\,\mathrm{meas}(\Omega_i), \quad i = 1,\dots,n_{\rm b}. \tag{7}$$

Now, in order to take into account the motion of the machine, we split the domain Ω into two parts, $\Omega^{\rm rot}$ and $\Omega^{\rm sta}$ separated by a circumference Γ strictly contained in the air-gap. Therefore, domains $\Omega_{\rm mc}$ and Ω_0 are split into two parts as well, one of them included in the rotor ($\Omega^{\rm rot}_{\rm mc}$ and $\Omega^{\rm rot}_0$) and the other one in the stator ($\Omega^{\rm sta}_{\rm mc}$ and $\Omega^{\rm sta}_0$). Notice that each of the two parts in which the airgap is also divided has been included in the corresponding adjacent subdomain $\Omega^{\rm rot}_0$ or $\Omega^{\rm sta}_0$. Thus, for the initial position of the motor, we can write

$$\Omega^{\rm rot} = \mathrm{int}\left(\overline{\Omega^{\rm rot}_0} \cup \left(\bigcup_{i=1}^{n_{\rm b}} \overline{\Omega_i}\right) \cup \overline{\Omega^{\rm rot}_{\rm mc}}\right), \quad \Omega^{\rm sta} = \mathrm{int}\left(\overline{\Omega^{\rm sta}_0} \cup \left(\bigcup_{i=n_{\rm b}+1}^{n_{\rm c}} \overline{\Omega_i}\right) \cup \overline{\Omega^{\rm sta}_{\rm mc}}\right).$$

In the case of moving bodies, Ohm's law (4) changes (see [14] for a short presentation). However, we consider a reference frame moving with the rotor so that, in this particular frame, $\Omega^{\rm rot}$ is fixed and $\Omega^{\rm sta}$ is moving. As a consequence, equations (7) remain valid. We notice that, in the framework of induction machines, a usual solution is working with Lagrangian coordinates in both rotor and stator (see, for instance, [15, 3, 16]). However, in our case, it is enough to consider a unique reference system moving with the rotor as the conductors present in the stator are stranded conductors and their respective currents are known. Therefore, neither Ohm's law (4) nor Faraday's law (2) are needed to state the problem in the domain corresponding to the stator.

If we call r_t the rotation whose angular velocity is the opposite to the one of the rotor the stator has a different position with respect to the initial time, given by $r_t\left(\Omega^{\rm sta}\right)$.

It is important to notice that both the rotor and stator geometric sets, $\Omega^{\rm rot}$ and $\Omega^{\rm sta}$, are always the same, but the physical parameters at each point may change along the time as they are not invariant with respect to rotation r_t.

In what follows, we will denote by $[\cdot]_\Gamma$ the jump across interface Γ. Thus, in terms of A_z, the transient magnetic model reads:

$$-\,\mathrm{div}(\nu(x,y;|\mathbf{grad}\, A_z|)\,\mathbf{grad}\, A_z) = \sum_{i=1}^{n_{\rm b}} \frac{y_i(t)}{\mathrm{meas}(\Omega_i)}\chi_{\Omega_i} \quad \text{in } \Omega^{\rm rot}, \tag{8}$$

$$-\,\mathrm{div}(\nu(x,y;|\mathbf{grad}\, A_z|)\,\mathbf{grad}\, A_z) = \sum_{i=n_{\rm b}+1}^{n_{\rm c}} \frac{I_i(t)}{\mathrm{meas}(\Omega_i)}\chi_{r_t(\Omega_i)} \quad \text{in } r_t\left(\Omega^{\rm sta}\right), \tag{9}$$

$$[A_z]_\Gamma = 0, \tag{10}$$

$$[\nu_0\,\mathbf{grad}\, A_z \cdot \mathbf{n}]_\Gamma = 0, \tag{11}$$

$$\frac{d}{dt}\int_{\Omega_i} \sigma A_z(x,y,t)\,dxdy + y_i(t) = -C_i(t)\sigma\,\mathrm{meas}(\Omega_i), \quad i = 1,\dots,n_{\rm b}, \tag{12}$$

where χ_D is the characteristic function of subset D. Notice that the interface conditions (10)-(11) guarantee the continuity of $\boldsymbol{B}\cdot\boldsymbol{n}$ and $\boldsymbol{H}\times\boldsymbol{n}$ through the interface separating rotor and stator. Moreover, on boundary

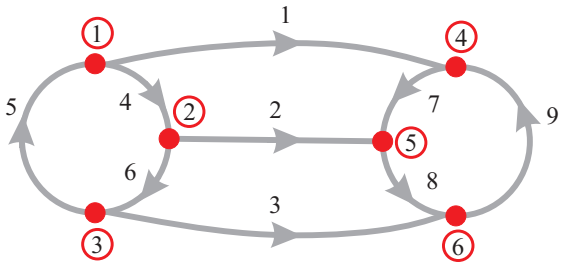

$$\mathcal{A} = \begin{pmatrix} -1 & 0 & 0 & -1 & 1 & 0 & 0 & 0 & 0 \\ 0 & -1 & 0 & 1 & 0 & -1 & 0 & 0 & 0 \\ 0 & 0 & -1 & 0 & -1 & 1 & 0 & 0 & 0 \\ 1 & 0 & 0 & 0 & 0 & 0 & -1 & 0 & 1 \\ 0 & 1 & 0 & 0 & 0 & 0 & 1 & -1 & 0 \\ 0 & 0 & 1 & 0 & 0 & 0 & 0 & 1 & -1 \end{pmatrix}$$

Figure 3: Example of graph topology and associated incidence matrix.

$\partial\Omega$ we consider the homogeneous Dirichlet boundary condition $A_z = 0$, which ensures $\boldsymbol{B} \cdot \boldsymbol{n} = 0$ on $\partial\Omega$.

As we mentioned before, the magnetic field in the squirrel cage is induced by the one in the stator. Therefore, neither currents $y_i(t)$ nor potential drops per unit length $C_i(t)$, $i = 1, \ldots, n_{\mathrm{b}}$, are known in advance. To be able to compute them, we have to take into account that all bars are connected to each other through the end-rings. Since we cannot include these end-rings in the 2D model of the cross-section of the motor, we will write a lumped model for the squirrel cage electrical circuit to be coupled with the distributed one. The topology of this circuit is modelled as a directed graph. Let us recall that the incidence matrix of a directed graph is the $n_{\mathrm{nod}} \times n_{\mathrm{edg}}$ (nodes by edges) matrix $\mathcal{A} = (a_{ij})$ defined by

$$a_{ij} = \begin{cases} -1 & \text{if } i = m(1, j), \\ 1 & \text{if } i = m(2, j), \\ 0 & \text{otherwise,} \end{cases}$$

for $i \in \{1, \ldots, n_{\mathrm{nod}}\}$, $j \in \{1, \ldots, n_{\mathrm{edg}}\}$, where $m(1, j)$, $m(2, j)$ denote the first and second nodes of the j-th edge, respectively. A simple example is shown in Figure 3 where the number of nodes is $n_{\mathrm{nod}} = 6$ and the number of edges $n_{\mathrm{edg}} = 9$. We notice that for a symmetric squirrel cage like the one schematized in Figure 3, we have, $n_{\mathrm{nod}} = 2n_{\mathrm{b}}$ and $n_{\mathrm{edg}} = 3n_{\mathrm{b}}$. We also notice that, in order for the lumped model to be coherent with the distributed one, the edges corresponding to the rotor bars have to be oriented in the positive z-direction. Moreover, in order to fix the notation, we advance that we are going to number the edges of the graph corresponding to the rotor bars in the first place. Besides, the nodes of the graph will be numbered in such a way that all nodes corresponding to one of the rings go first, followed by those of the other ring.

By using the incidence matrix, the first Kirchhoff's law can be written as follows:

$$\mathcal{A}\vec{y}(t) = \vec{0}, \tag{13}$$

where $\vec{y}(t) \in \mathbb{R}^{n_{\mathrm{edg}}}$ denotes the vector of currents along the edges of the graph. Let us introduce the vector of nodal electric potentials at time t, denoted by $\vec{v}(t) \in \mathbb{R}^{n_{\mathrm{nod}}}$, and the resistance of the i-th bar per unit length in the z spatial direction denoted by

$$\alpha_i := \frac{1}{\sigma \operatorname{meas}(\Omega_i)},$$

$i = 1, \ldots, n_{\mathrm{b}}$. Then, the constitutive equations for the circuit elements can be written as (see, for instance, [17])

$$\mathcal{D}\vec{y}(t) + \mathcal{A}^{\top}\vec{v}(t) = \vec{0}, \tag{14}$$

where $\mathcal{D}$ denotes the diagonal operator given by $(\mathcal{D}\vec{y}(t))_i = \mathcal{D}_i(y_i(t))$, with

$$\mathcal{D}_i(y_i(t)) = \begin{cases} R_i \dfrac{d}{dt} \displaystyle\int_{\Omega_i} \sigma A_z(t) + R_i y_i(t) & i = 1, \ldots, n_{\mathrm{b}}, \\ R_i y_i(t) & i = n_{\mathrm{b}} + 1, \ldots, n_{\mathrm{edg}}, \end{cases}$$

R_i, $i = n_\mathrm{b}+1, \ldots, n_\mathrm{edg}$, being the resistance of the i-th edge of the graph, and $R_i = \ell_i \alpha_i$, $i = 1, \ldots, n_\mathrm{b}$, the resistance of the i-th rotor bar with ℓ_i its length. We notice that expressions for $\mathcal{D}_i\left(y_i(t)\right)$, $i = 1, \ldots, n_\mathrm{b}$, are obtained similarly to (7).

Thus, the problem to be solved is the following:

Problem 1. *Given currents along the coil sides, $I_i(t)$, $i = n_\mathrm{b}+1, \ldots, n_\mathrm{c}$, and a vector of initial currents along the bars, $\vec{y}^{\,b,0} = (y_1^0, \ldots, y_{n_\mathrm{b}}^0)$, find, for every $t \in [0,T]$, a field $A_z(x,y,t)$, currents along the edges of the graph, $y_i(t)$, $i = 1, \ldots, n_\mathrm{edg}$, and voltages at the nodes of the graph, $v_i(t)$, $i = 1, \ldots, n_\mathrm{nod}$, such that*

$$-\operatorname{div}(\nu(x,y;|\mathbf{grad}\, A_z|)\,\mathbf{grad}\, A_z) = \sum_{i=1}^{n_\mathrm{b}} \frac{y_i(t)}{\operatorname{meas}(\Omega_i)}\chi_{\Omega_i} \quad \text{in } \Omega^\mathrm{rot}, \tag{15}$$

$$-\operatorname{div}(\nu(x,y;|\mathbf{grad}\, A_z|)\,\mathbf{grad}\, A_z) = \sum_{i=n_\mathrm{b}+1}^{n_\mathrm{c}} \frac{I_i(t)}{\operatorname{meas}(\Omega_i)}\chi_{r_t(\Omega_i)} \quad \text{in } r_t\left(\Omega^\mathrm{sta}\right), \tag{16}$$

$$[A_z]_\Gamma = 0, \tag{17}$$

$$[\nu_0\, \mathbf{grad}\, A_z \cdot \mathbf{n}]_\Gamma = 0, \tag{18}$$

$$A_z = 0 \quad \text{on } \partial\Omega, \tag{19}$$

$$\mathcal{D}\vec{y}(t) + \mathcal{A}^\top \vec{v}(t) = \vec{0}, \tag{20}$$

$$\mathcal{A}\vec{y}(t) = \vec{0}, \tag{21}$$

$$y_i(0) = y_i^0,\ i = 1, \ldots, n_\mathrm{b}. \tag{22}$$

To the authors' knowledge, the analysis of the field-circuit problem stated in Problem 1 has not been done in the literature. Regarding this question, we can cite the recent work [18] where the authors analyze a simplified coupled problem without motion, imposing the voltage drops in all conducting domains. We must also highlight reference [15] which deals with an eddy current problem including the motion of the machine, but restricted to the linear magnetic case and without circuit coupling.

3. A Reduced Problem

The goal of this section is to obtain an equivalent formulation to Problem 1 having the currents along the rotor bars as the only unknowns. For this purpose, let us first introduce some notations that will allow us to write Problem 1 in a more compact form. Let $\vec{\mathcal{F}} : [0,T] \times \mathbb{R}^{n_\mathrm{b}} \longrightarrow \mathbb{R}^{n_\mathrm{b}}$ be the nonlinear mapping defined as

$$\vec{\mathcal{F}}(t,\vec{w}) := \left(\int_{\Omega_1} \sigma A_z(x,y,t)\; dx\, dy, \ldots, \int_{\Omega_{n_\mathrm{b}}} \sigma A_z(x,y,t)\; dx\, dy \right)^\top \in \mathbb{R}^{n_\mathrm{b}},$$

with $A_z(x,y,t)$ the solution to the following nonlinear magnetostatic problem:

Problem 2. *Given a fixed $t \in [0,T]$, currents along the coil sides $I_i(t)$, $i = n_\mathrm{b}+1, \ldots, n_\mathrm{c}$, and $\vec{w} \in \mathbb{R}^{n_\mathrm{b}}$,*

find a field $A_z(x,y,t)$ *such that*

$$-\operatorname{div}(\nu(x,y;|\mathbf{grad}\,A_z|)\,\mathbf{grad}\,A_z) = \sum_{i=1}^{n_\mathrm{b}} \frac{w_i}{\operatorname{meas}(\Omega_i)}\chi_{\Omega_i} \quad \textit{in } \Omega^{\mathrm{rot}}, \tag{23}$$

$$-\operatorname{div}(\nu(x,y;|\mathbf{grad}\,A_z|)\,\mathbf{grad}\,A_z) = \sum_{i=n_\mathrm{b}+1}^{n_\mathrm{c}} \frac{I_i(t)}{\operatorname{meas}(\Omega_i)}\chi_{r_t(\Omega_i)} \quad \textit{in } r_t\left(\Omega^{\mathrm{sta}}\right), \tag{24}$$

$$[A_z]_\Gamma = 0, \tag{25}$$

$$[\nu_0\,\mathbf{grad}\,A_z\cdot\mathbf{n}]_\Gamma = 0, \tag{26}$$

$$A_z = 0 \quad \textit{on } \partial\Omega. \tag{27}$$

This is a nonlinear magnetostatic problem for each time $t>0$. We refer the reader to [19] for the analysis of nonlinear magnetostatic problems defined on fixed domains.

Notice that two blocks can be distinguished in equation (20), one corresponding to the rotor bars and another one corresponding to the remaining edges of the squirrel cage, namely, those of the end-rings. Let us denote the incidence matrices of their respective subgraphs by $\mathcal{A}^b$ $(n_{\mathrm{nod}}\times n_\mathrm{b})$ and $\mathcal{A}^r$ $(n_{\mathrm{nod}}\times(n_{\mathrm{edg}}-n_\mathrm{b}))$; notice that, in terms of n_b, the dimensions of $\mathcal{A}^b$ and $\mathcal{A}^r$ are $2n_\mathrm{b}\times n_\mathrm{b}$ and $2n_\mathrm{b}\times 2n_\mathrm{b}$, respectively. Thus, we have $\mathcal{A}=\left(\mathcal{A}^b \mid \mathcal{A}^r\right)$, and, accordingly, the vector of currents $\vec{y}$ is decomposed as

$$\vec{y} = \begin{pmatrix} \vec{y}^{\,b} \\ \vec{y}^{\,r} \end{pmatrix}.$$

Then, equation (20) can be rewritten as

$$\mathcal{R}^b\frac{d}{dt}\vec{\mathcal{F}}\left(t,\vec{y}^{\,b}(t)\right) + \mathcal{R}^b\vec{y}^{\,b}(t) + \left(\mathcal{A}^b\right)^\top\vec{v}(t) = \vec{0}, \tag{28}$$

$$\mathcal{R}^r\vec{y}^{\,r}(t) + \left(\mathcal{A}^r\right)^\top\vec{v}(t) = \vec{0}, \tag{29}$$

where $\mathcal{R}^b$ and $\mathcal{R}^r$ are the diagonal matrices defined by

$$\begin{aligned} \left(\mathcal{R}^b\right)_{ij} &= R_i\delta_{ij}, \qquad i,j=1,\dots,n_\mathrm{b},\\ \left(\mathcal{R}^r\right)_{ij} &= R_{i+n_\mathrm{b}}\delta_{ij}, \quad i,j=1,\dots,n_{\mathrm{edg}}-n_\mathrm{b}, \end{aligned}$$

with δ_{ij} the Kronecker delta, that is,

$$\delta_{ij} = \begin{cases} 0 & \text{if } i\neq j,\\ 1 & \text{if } i=j. \end{cases}$$

Notice that (28) involves operator $\vec{\mathcal{F}}$ which is defined in terms of $I_i(t)$, $i=n_\mathrm{b}+1,\dots,n_\mathrm{c}$, through the solution of Problem 2. Thus, equations (15)–(21) can be rewritten in the more compact manner,

$$\mathcal{R}^b\frac{d}{dt}\vec{\mathcal{F}}\left(t,\vec{y}^{\,b}(t)\right) + \mathcal{R}^b\vec{y}^{\,b}(t) + \left(\mathcal{A}^b\right)^\top\vec{v}(t) = \vec{0}, \tag{30}$$

$$\mathcal{R}^r\vec{y}^{\,r}(t) + \left(\mathcal{A}^r\right)^\top\vec{v}(t) = \vec{0}, \tag{31}$$

$$\mathcal{A}^b\vec{y}^{\,b}(t) + \mathcal{A}^r\vec{y}^{\,r}(t) = \vec{0}. \tag{32}$$

Moreover, since $\mathcal{R}^r$ is a non-singular matrix, from (31) we get

$$\vec{y}^{\,r}(t) = -\left(\mathcal{R}^r\right)^{-1}\left(\mathcal{A}^r\right)^\top\vec{v}(t),$$

and thus $\vec{y}^{\,r}$ can be eliminated from the above system. Therefore, Problem 1 can be written in the following way:

Problem 3. *Given currents along the coil sides $I_i(t)$, $i = n_{\rm b}+1, \dots, n_{\rm c}$, and initial currents along the bars $\vec{y}^{\,b,0} = (y_1^0, \dots, y_{n_{\rm b}}^0)$, find, for every $t \in [0,T]$, currents ${y_i}^b(t)$, $i = 1, \dots, n_{\rm b}$, along the bars and voltages $v_i(t)$, $i = 1, \dots, n_{\rm nod}$, at the nodes of the graph such that*

$$\mathcal{R}^b \frac{d}{dt}\vec{\mathcal{F}}\left(t, \vec{y}^{\,b}(t)\right) + \mathcal{R}^b \vec{y}^{\,b}(t) + \left(\mathcal{A}^b\right)^\top \vec{v}(t) = \vec{0}, \tag{33}$$

$$\mathcal{A}^b \vec{y}^{\,b}(t) - \mathcal{A}^r (\mathcal{R}^r)^{-1} \left(\mathcal{A}^r\right)^\top \vec{v}(t) = \vec{0}, \tag{34}$$

$$\vec{y}^{\,b}(0) = \vec{y}^{\,b,0}, \tag{35}$$

where mapping $\vec{\mathcal{F}}$ depends on the given currents in the coils, $I_i(t)$, $i = n_{\rm b}+1, \dots, n_{\rm c}$, through the solution of Problem 2.

Remark 4. *Problem 1 and Problem 3 are equivalent in the following sense: given currents along the coil sides $I_i(t)$, $i = n_{\rm b}+1, \dots, n_{\rm c}$, and initial currents along the bars $\vec{y}^{\,b,0} = (y_1^0, \dots, y_{n_{\rm b}}^0)$, for every $t \in [0,T]$ we have:*

i) If $A_z(x,y,t)$, $\vec{y}(t) \in \mathbb{R}^{n_{\rm edg}}$ and $\vec{v}(t) \in \mathbb{R}^{n_{\rm nod}}$ are solutions of Problem 1, then $\vec{y}^{\,b}(t)$ defined as $y_i^b(t) = y_i(t)$ for $i = 1, \dots, n_{\rm b}$ and $\vec{v}(t)$ are solutions of Problem 3.

ii) Reciprocally, for $t \in [0,T]$ let $\vec{y}^{\,b}(t) \in \mathbb{R}^{n_{\rm b}}$ and $\vec{v}(t) \in \mathbb{R}^{n_{\rm nod}}$ be solutions of Problem 3. Let us define $\vec{y}^{\,r}(t) := -(\mathcal{R}^r)^{-1}(\mathcal{A}^r)^\top \vec{v}(t)$, $\vec{y}(t) := (\vec{y}^{\,b} | \vec{y}^{\,r})^\top$ and let us also consider $A_z(x,y,t)$ the solution of Problem 2 with data $\vec{w} = \vec{y}^{\,b}(t)$. Then, $A_z(x,y,t)$, $\vec{y}(t)$ and $\vec{v}(t)$ are solutions of Problem 1.

Statement i) is a direct consequence of the construction of Problem 3. Let us see the proof of ii). Multiplying $\vec{y}^{\,r}(t) := -(\mathcal{R}^r)^{-1}(\mathcal{A}^r)^\top \vec{v}(t)$ by $\mathcal{R}^r$ we have

$$\mathcal{R}^r \vec{y}^{\,r}(t) + \left(\mathcal{A}^r\right)^\top \vec{v}(t) = \vec{0}. \tag{36}$$

From (36), (33) *and the definition of $\mathcal{D}$ we obtain* (20).

On the other hand, by replacing the definition of $\vec{y}^{\,r}$ in (34) *we clearly obtain*

$$\mathcal{A}^b \vec{y}^{\,b}(t) + \mathcal{A}^r \vec{y}^{\,r}(t) = \vec{0}.$$

Consequently, $\vec{y}(t) = (\vec{y}^{\,b} | \vec{y}^{\,r})^\top$ satisfies (21). *Finally, equations* (15)-(19) *are an immediate consequence of the definition of $A_z(x,y,t)$ and the initial condition* (22) *is derived from* (35).

Next, we show that $\vec{v}(t)$ can be eliminated from system (33)-(34) although matrix $\mathcal{A}^r(\mathcal{R}^r)^{-1}\left(\mathcal{A}^r\right)^\top$ in (34) is not invertible.

Lemma 5. *If the currents along the bars, $y_i^b(t)$, $i = 1, \dots, n_{\rm b}$, are such that*

$$\mathcal{A}^b \vec{y}^{\,b}(t) \cdot \begin{pmatrix} \vec{0} \\ \vec{e} \end{pmatrix} = 0, \tag{37}$$

with $\vec{e} = (1, \dots, 1)^\top \in \mathbb{R}^{n_{\rm b}}$, then there exist an invertible matrix $\mathcal{B}$ and a scalar function $\lambda(t)$ such that

$$\vec{v}(t) = \mathcal{B}^{-1}\mathcal{A}^b \vec{y}^{\,b}(t) + \lambda(t) \begin{pmatrix} \vec{0} \\ \vec{e} \end{pmatrix}.$$

Proof. Let us start by analyzing the nullspace of matrix $\left(\mathcal{A}^r\right)^\top$. Firstly, since the graph corresponding to the whole squirrel cage is connected, we have

$$\mathrm{N}\left(\left(\mathcal{A}\right)^\top\right) = < \begin{pmatrix} \vec{e} \\ \vec{e} \end{pmatrix} >, \tag{38}$$

where the notation $< \vec{u}_1, \vec{u}_2, \ldots, \vec{u}_n >$ stands for the span of $\{\vec{u}_1, \vec{u}_2, \ldots, \vec{u}_n\}$. Similarly, since the subgraph obtained by removing the bars has two connected components (the two end-rings), each of them having $n_{\rm b}$ nodes, the rank of matrix $\mathcal{A}^r$ is $2n_{\rm b}-2$ (see Theorem 7.2 in [20]). Therefore, we conclude that the dimension of the nullspace of $(\mathcal{A}^r)^\top$ is two. If we number the nodes of one of the rings first and then the nodes of the other ring, this nullspace is given by

$$\mathrm{N}\left((\mathcal{A}^r)^\top\right) = < \begin{pmatrix} \vec{e} \\ \vec{0} \end{pmatrix}, \begin{pmatrix} \vec{0} \\ \vec{e} \end{pmatrix} > .$$

Moreover, it is easy to prove that

$$\mathrm{N}\left(\mathcal{A}^r(\mathcal{R}^r)^{-1}(\mathcal{A}^r)^\top\right) = \mathrm{N}\left((\mathcal{A}^r)^\top\right).$$

Indeed, it is obvious that $\mathrm{N}((\mathcal{A}^r)^\top) \subset \mathrm{N}(\mathcal{A}^r(\mathcal{R}^r)^{-1}(\mathcal{A}^r)^\top)$. Conversely, if $\vec{z} \in \mathrm{N}(\mathcal{A}^r(\mathcal{R}^r)^{-1}(\mathcal{A}^r)^\top)$, we have,

$$0 = \mathcal{A}^r(\mathcal{R}^r)^{-1}(\mathcal{A}^r)^\top \vec{z} \cdot \vec{z} = (\mathcal{R}^r)^{-1}(\mathcal{A}^r)^\top \vec{z} \cdot (\mathcal{A}^r)^\top \vec{z}$$

and, since the linear transformation associated to $(\mathcal{R}^r)^{-1}$ is bijective, we conclude that $\vec{z}$ also belongs to $\mathrm{N}((\mathcal{A}^r)^\top)$.

Thus, from well-known results in linear algebra, the linear mapping

$$\widetilde{\mathcal{A}^r(\mathcal{R}^r)^{-1}(\mathcal{A}^r)^\top} : \mathbb{R}^{2n_{\rm b}}/\mathrm{N}\left((\mathcal{A}^r)^\top\right) \to \mathrm{Im}\left(\mathcal{A}^r(\mathcal{R}^r)^{-1}(\mathcal{A}^r)^\top\right)$$

is an isomorphism, where $\widetilde{\mathcal{A}^r(\mathcal{R}^r)^{-1}(\mathcal{A}^r)^\top}$ is well-defined by

$$\widetilde{\mathcal{A}^r(\mathcal{R}^r)^{-1}(\mathcal{A}^r)^\top}(\vec{w} + \mathrm{N}\left((\mathcal{A}^r)^\top\right)) := \mathcal{A}^r(\mathcal{R}^r)^{-1}(\mathcal{A}^r)^\top \vec{w}, \quad \forall \vec{w} \in \mathbb{R}^{2n_{\rm b}}.$$

Therefore, if $\mathcal{A}^b\vec{y}^b(t) \in \mathrm{Im}\left(\mathcal{A}^r(\mathcal{R}^r)^{-1}(\mathcal{A}^r)^\top\right)$, there exists a unique $\vec{v}(t)$ in the quotient space $\mathbb{R}^{2n_{\rm b}}/\mathrm{N}\left((\mathcal{A}^r)^\top\right)$ solution of (34). Firstly, let us characterize $\mathrm{Im}\left(\mathcal{A}^r(\mathcal{R}^r)^{-1}(\mathcal{A}^r)^\top\right)$. We have,

$$\mathrm{Im}\left(\mathcal{A}^r(\mathcal{R}^r)^{-1}(\mathcal{A}^r)^\top\right) = \mathrm{N}\left(\mathcal{A}^r(\mathcal{R}^r)^{-1}(\mathcal{A}^r)^\top\right)^\perp = \mathrm{N}\left((\mathcal{A}^r)^\top\right)^\perp = < \begin{pmatrix} \vec{\mathrm{e}} \\ \vec{0} \end{pmatrix}, \begin{pmatrix} \vec{0} \\ \vec{\mathrm{e}} \end{pmatrix} >^\perp .$$

Now, let us notice that the assumption (37) is equivalent to the following conditions

$$\vec{y}^b \perp (\mathcal{A}^b)^\top \begin{pmatrix} \vec{e} \\ \vec{0} \end{pmatrix}, \tag{39}$$

$$\vec{y}^b \perp (\mathcal{A}^b)^\top \begin{pmatrix} \vec{0} \\ \vec{e} \end{pmatrix}. \tag{40}$$

Indeed, taking into account (38) we have

$$\vec{0} = (\mathcal{A})^\top \begin{pmatrix} \vec{e} \\ \vec{e} \end{pmatrix} = \begin{pmatrix} (\mathcal{A}^b)^\top \\ (\mathcal{A}^r)^\top \end{pmatrix} \begin{pmatrix} \vec{e} \\ \vec{e} \end{pmatrix} = \begin{pmatrix} (\mathcal{A}^b)^\top \begin{pmatrix} \vec{e} \\ \vec{e} \end{pmatrix} \\ (\mathcal{A}^r)^\top \begin{pmatrix} \vec{e} \\ \vec{e} \end{pmatrix} \end{pmatrix},$$

and then

$$\vec{0} = (\mathcal{A}^b)^\top \begin{pmatrix} \vec{e} \\ \vec{e} \end{pmatrix} = (\mathcal{A}^b)^\top \begin{pmatrix} \vec{e} \\ \vec{0} \end{pmatrix} + (\mathcal{A}^b)^\top \begin{pmatrix} \vec{0} \\ \vec{e} \end{pmatrix}.$$

Consequently, if (40) holds (39) also holds.

Therefore, the assumption (37) guarantees that $\mathcal{A}^b\vec{y}^b(t)$ belongs to $\mathrm{Im}(\mathcal{A}^r(\mathcal{R}^r)^{-1}(\mathcal{A}^r)^\top)$ and we can solve equation (34) to get

$$\hat{v}(t) = \left(\mathcal{A}^r\widetilde{(\mathcal{R}^r)^{-1}}(\mathcal{A}^r)^\top\right)^{-1}\mathcal{A}^b\vec{y}^b(t) \in \mathbb{R}^{2n_\mathrm{b}}/\mathrm{N}\left((\mathcal{A}^r)^\top\right).$$

We know that $\vec{v}(t) \in \hat{v}(t)$ so there are two free parameters that have to be determined to compute $\vec{v}(t)$, as two is the dimension of the nullspace $\mathrm{N}((\mathcal{A}^r)^\top)$. Let $\vec{w}(t)$ be any element in $\hat{v}(t)$. Then

$$\vec{v}(t) = \vec{w}(t) + \phi(t)\begin{pmatrix}\vec{e}\\ \vec{0}\end{pmatrix} + \lambda(t)\begin{pmatrix}\vec{0}\\ \vec{e}\end{pmatrix},$$

for any choice of $\phi(t)$ and $\lambda(t)$. Since the potential is defined up to a constant, we can arbitrarily choose either $\phi(t)$ or $\lambda(t)$. For instance, if we take $\phi(t) = 0$, $\lambda(t)$ is an unknown of the problem that is determined by condition

$$\mathcal{A}^b\vec{y}^b(t)\cdot\begin{pmatrix}\vec{0}\\ \vec{e}\end{pmatrix} = 0.$$

Now, we are going to build a particular solution $\vec{w}(t)$. To attain this goal, let us denote by $\mathcal{E}$ the matrix of order $2n_\mathrm{b}\times(2n_\mathrm{b}-2)$ whose columns span $\mathrm{N}((\mathcal{A}^r)^\top)^\perp$. Since $\mathrm{N}((\mathcal{A}^r)^\top)^\perp = \mathrm{Im}(\mathcal{A}^r)$, matrix $\mathcal{E}$ can be obtained from matrix $\mathcal{A}^r$ by eliminating two columns, each corresponding to an edge of each end-ring.

It is easy to see that $\mathcal{E}^\top\mathcal{A}^r(\mathcal{R}^r)^{-1}\left(\mathcal{A}^r\right)^\top\mathcal{E}$ is an invertible matrix of order $2n_\mathrm{b}-2$. By using this matrix, we define the vector $\vec{w}(t)$ as

$$\vec{w}(t) := \mathcal{E}(\mathcal{E}^\top\mathcal{A}^r(\mathcal{R}^r)^{-1}\left(\mathcal{A}^r\right)^\top\mathcal{E})^{-1}\mathcal{E}^\top\mathcal{A}^b\vec{y}^b(t).$$

Next, we are going to proof that $\vec{w}(t) \in \hat{v}(t)$. We have

$$\begin{aligned}&\mathcal{E}^\top\mathcal{A}^r(\mathcal{R}^r)^{-1}\left(\mathcal{A}^r\right)^\top\vec{w}(t)\\ &\qquad= \mathcal{E}^\top\mathcal{A}^r(\mathcal{R}^r)^{-1}\left(\mathcal{A}^r\right)^\top\mathcal{E}(\mathcal{E}^\top\mathcal{A}^r(\mathcal{R}^r)^{-1}\left(\mathcal{A}^r\right)^\top\mathcal{E})^{-1}\mathcal{E}^\top\mathcal{A}^b\vec{y}^b(t) = \mathcal{E}^\top\mathcal{A}^b\vec{y}^b(t)\end{aligned} \quad (41)$$

and, since $\mathcal{E}^\top$ is one-to-one on $\mathrm{Im}(\mathcal{A}^r(\mathcal{R}^r)^{-1}\left(\mathcal{A}^r\right)^\top)$, (41) implies

$$\mathcal{A}^r(\mathcal{R}^r)^{-1}\left(\mathcal{A}^r\right)^\top\vec{w}(t) = \mathcal{A}^b\vec{y}^b(t).$$

Finally, we conclude the lemma for

$$\mathcal{B} := \left(\mathcal{E}(\mathcal{E}^\top\mathcal{A}^r(\mathcal{R}^r)^{-1}\left(\mathcal{A}^r\right)^\top\mathcal{E})^{-1}\mathcal{E}^\top\right)^{-1}.$$

□

Remark 6. *Since $\vec{w}(t)$ is any element in $\hat{v}(t)$, instead of building matrix $\mathcal{B}^{-1}$, $\vec{w}$ could also be obtained by blocking two particular degrees of freedom, each corresponding to one node of each ring of the squirrel cage, when solving the otherwise singular linear system*

$$\mathcal{A}^r(\mathcal{R}^r)^{-1}\left(\mathcal{A}^r\right)^\top\vec{v}(t) = \mathcal{A}^b\vec{y}^b(t).$$

Thanks to the above lemma, the problem to be solved can be written in terms of $\vec{y}^b(t)$ and $\lambda(t)$ as follows:

Problem 7. *Given currents along the coil sides $I_i(t)$, $i = n_{\rm b}+1, \ldots, n_{\rm c}$, and initial currents along the bars $\vec{y}^{\,b,0} = (y_1^0, \ldots, y_{n_{\rm b}}^0)$, find, for every $t \in [0,T]$, currents ${y_i}^b(t)$, $i = 1, \ldots, n_{\rm b}$, along the bars and $\lambda(t) \in \mathbb{R}$ such that*

$$\mathcal{R}^b \frac{d}{dt}\vec{\mathcal{F}}\left(t, \vec{y}^{\,b}(t)\right) + \left(\mathcal{R}^b + \left(\mathcal{A}^b\right)^\top \mathcal{B}^{-1}\left(\mathcal{A}^b\right)\right)\vec{y}^{\,b}(t) + \lambda(t)\left(\mathcal{A}^b\right)^\top \begin{pmatrix} \vec{0} \\ \vec{e} \end{pmatrix} = \vec{0}, \tag{42}$$

$$\mathcal{A}^b \vec{y}^{\,b}(t) \cdot \begin{pmatrix} \vec{0} \\ \vec{e} \end{pmatrix} = 0, \tag{43}$$

$$\vec{y}^{\,b}(0) = \vec{y}^{\,b,0}, \tag{44}$$

where mapping $\vec{\mathcal{F}}$ depends on the given currents in the coils, $I_i(t)$, $i = n_{\rm b}+1, \ldots, n_{\rm c}$, through the solution of Problem 2

4. An Approximate Method to Compute Appropriate Initial Currents in Rotor Bars

In this section, we propose a method to compute an approximation of the initial condition of Problem 7 corresponding to a periodic steady solution, under the assumption that currents along the stator coil sides are periodic functions of the same frequency f_c. In order to compute this solution, we could take any initial condition vector $\vec{y}^{\,b,0} = (y_1^0, \ldots, y_{n_{\rm b}}^0)$, (null, for instance), and integrate the differential-algebraic system of equations given above until convergence. However, this procedure can be very costly from the computational point of view if the initial currents are far from the ones corresponding to the periodic solution we are looking for. The aim is to determine these initial currents in such a way that the periodic steady solution can be obtained by integrating the problem along a time-interval as small as possible.

Firstly, we will introduce some notation. Let us assume that the rotor is moving at a constant angular velocity n_r (in rpm). Also, let n_s be the so-called synchronous speed (that is, the rotation rate of the magnetic field in the stator), which is given by $n_s = (60 f_c)/p$ (in rpm), p being the number of pole-pairs of the machine. Furthermore, let s be the slip, that is, the difference between synchronous and operating speed, relative to the synchronous speed, $s = (n_s - n_r)/n_s$. Then, one can prove that the period of the current in the bars, T_b, is such that $T_b = T_c/s$, where T_c denotes the electrical period of the stator coils (see, for instance, [21]).

If we successively integrate (42) first in $[0,t]$ and then in $[0,T_b]$ and we change the order of integration in the last two terms, we obtain

$$\mathcal{R}^b\left(\int_0^{T_b} \vec{\mathcal{F}}\left(t, \vec{y}^{\,b}(t)\right)\, dt - T_b \vec{\mathcal{F}}\left(0, \vec{y}^{\,b,0}\right)\right) + \left(\mathcal{R}^b + (\mathcal{A}^b)^\top \mathcal{B}^{-1}(\mathcal{A}^b)\right)\int_0^{T_b} (T_b - t)\vec{y}^{\,b}(t)\, dt + \left(\int_0^{T_b} (T_b - t)\lambda(t)\, dt\right)(\mathcal{A}^b)^\top \begin{pmatrix} \vec{0} \\ \vec{e} \end{pmatrix} = \vec{0}. \tag{45}$$

Now, we first conjecture that the leftmost term in (45), namely,

$$\mathcal{R}^b \int_0^{T_b} \vec{\mathcal{F}}\left(t, \vec{y}^{\,b}(t)\right)\, dt$$

can be neglected because, in real situations, it seems to be much smaller than the other terms. This can be seen for the particular example shown in Figure 4. From a physical point of view, this assumption means that the flux linkages of the rotor bars have approximately zero mean over one period of the fundamental

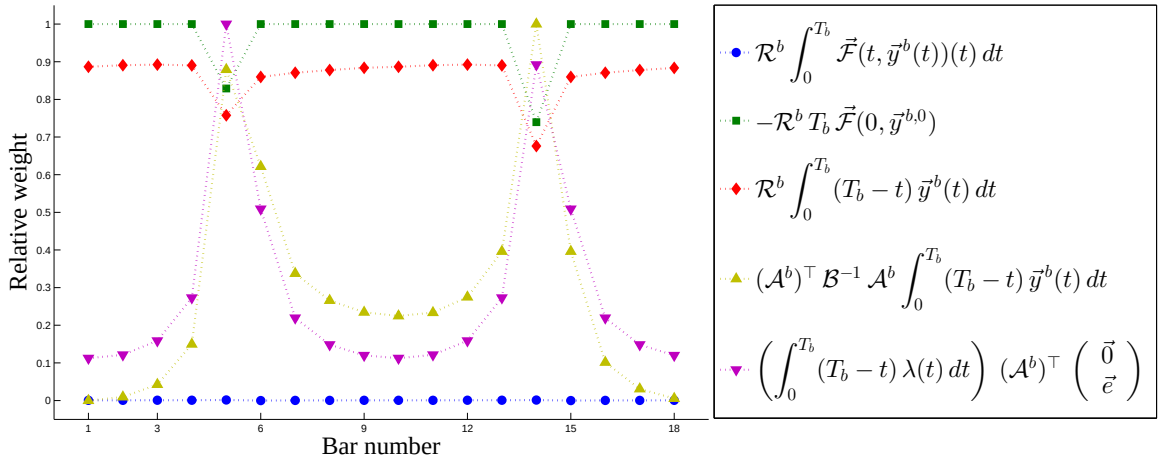

Figure 4: Relative value of the different terms in equation (45) versus the bar number.

frequency of currents in the rotor bars. Let us notice, however, that the term involving the resistances, namely,

$$\left(\mathcal{R}^b + (\mathcal{A}^b)^\top \mathcal{B}^{-1} \mathcal{A}^b\right) \int_0^{T_b} (T_b - t) \vec{y}^b(t)\, dt$$

cannot be neglected (see again Figure 4).

On the other hand, we would also like to avoid the calculation of $\vec{y}^b(t)$ because it is very expensive. Indeed, notice that at each iteration of any iterative algorithm solving (43)–(45), the computation of $\vec{y}^b(t)$ starting from $\vec{y}^{b,0}$ would involve the solution to the full model along the interval $[0, T_b]$. In order to avoid such a drawback, we notice that the currents along the rotor bars can be approximated by a harmonic function of frequency $f_b := 1/T_b$ (see Figure 5). This is a key point in the proposed technique because it allows us to approximate the original problem by means of a time-independent one. Moreover, for symmetry reasons, we will assume the amplitudes of the approximations of the currents in the rotor bars to be the same in all of them, which will be denoted by Y. Then, the idea is to approximate the vector of rotor bar currents, $\vec{y}^b(t)$, as follows:

$$y_i^b(t) \simeq \left[(\mathcal{A}^b)^\top \begin{pmatrix} \vec{0} \\ \vec{e} \end{pmatrix}\right]_i Y \cos(2\pi f_b t + \beta_i), \tag{46}$$

where β_i is the phase-shift between the current source in the coil sides and the current of the i-th bar. Accordingly, the initial currents are given by,

$$y_i^{b,0} = Y \left[(\mathcal{A}^b)^\top \begin{pmatrix} \vec{0} \\ \vec{e} \end{pmatrix}\right]_i \cos\beta_i. \tag{47}$$

On the other hand, from periodicity arguments one can show that the phase angles are

$$\beta_i = \beta_1 + (i-1)\gamma, \quad i = 1, \ldots, n_\mathrm{b}, \tag{48}$$

with $\gamma = (2\pi p)/n_\mathrm{b}$, and then only two unknowns remain: Y and β_1. In order to compute them we will construct a system of n_b nonlinear equations that will be solved in the least-square sense.

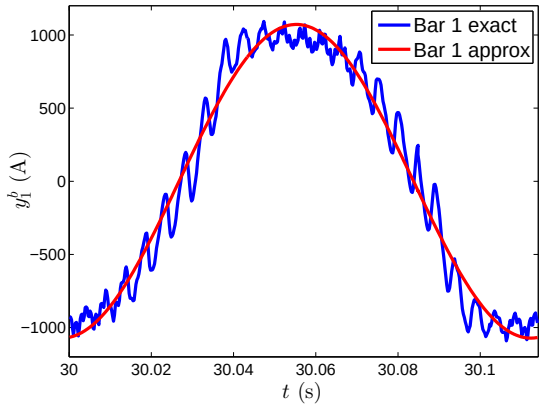

Figure 5: Comparison between $y_1^b(t)$ and the approximation given in (46).

Let us introduce the column vectors $\vec{u}$ and $\vec{w}$, whose respective i-th components are

$$u_i := \left[(\mathcal{A}^b)^\top \begin{pmatrix} \vec{0} \\ \vec{e} \end{pmatrix}\right]_i \cos\beta_i \quad \text{and} \quad w_i := \left[(\mathcal{A}^b)^\top \begin{pmatrix} \vec{0} \\ \vec{e} \end{pmatrix}\right]_i \sin\beta_i,$$

$i = 1, \ldots, n_\mathrm{b}$. Then, $\vec{y}^{\,b,0} = Y\vec{u}$. We also observe that

$$\vec{u} = \frac{\partial \vec{w}}{\partial \beta_1} \quad \text{and} \quad \vec{w} = -\frac{\partial \vec{u}}{\partial \beta_1}. \tag{49}$$

Lemma 8. *If $p \neq kN_b$, $k \in \mathbb{N}$, the approximate currents introduced in* (46) *satisfy constraint* (43) *for any values of Y and β_1.*

Proof. Taking into account that

$$\left[(\mathcal{A}^b)^\top \begin{pmatrix} \vec{0} \\ \vec{e} \end{pmatrix}\right]_i = \pm 1,$$

for $i = 1, \ldots, n_\mathrm{b}$, depending on the orientation of the i-th edge, we have

$$\begin{aligned}
\vec{y}^{\,b}(t) \cdot (\mathcal{A}^b)^\top \begin{pmatrix} \vec{0} \\ \vec{e} \end{pmatrix} &\approx \sum_{i=1}^{n_\mathrm{b}} \left[(\mathcal{A}^b)^\top \begin{pmatrix} \vec{0} \\ \vec{e} \end{pmatrix}\right]_i^2 Y \cos(2\pi f_b t + \beta_i) \\
&= Y \sum_{i=1}^{n_\mathrm{b}} \cos(2\pi f_b t + \beta_i) = Y \mathrm{Re}\left(\sum_{i=1}^{n_\mathrm{b}} \mathrm{e}^{\,i(2\pi f_b t + \beta_1 + (i-1)\gamma)} \right) \\
&= Y \mathrm{Re}\left(\mathrm{e}^{\,i(2\pi f_b t + \beta_1)} \frac{\mathrm{e}^{\,i n_\mathrm{b}\gamma} - 1}{\mathrm{e}^{\,i\gamma} - 1} \right) \\
&= Y \mathrm{Re}\left(\mathrm{e}^{\,i(2\pi f_b t + \beta_1)} \frac{\mathrm{e}^{\,i2\pi p} - 1}{\mathrm{e}^{\,i\gamma} - 1} \right) \\
&= 0,
\end{aligned} \tag{50}$$

as long as γ is not an integer multiple of 2π (which would mean that p is a multiple of n_b), because $\mathrm{e}^{\,i2\pi p} = 1$ for all integer p. □

Now, let us compute the integral $\int_0^{T_b}(T_b-t)y_i^b(t)\,dt$ by using the approximation introduced in (46). We have

$$\begin{aligned}\int_0^{T_b}(T_b-t)y_i^b(t)\,dt &\approx \left[(\mathcal{A}^b)^\top\begin{pmatrix}\vec{0}\\ \vec{e}\end{pmatrix}\right]_i\int_0^{T_b}(T_b-t)Y\cos\left(\frac{2\pi}{T_b}t+\beta_i\right)dt\\ &= -\left[(\mathcal{A}^b)^\top\begin{pmatrix}\vec{0}\\ \vec{e}\end{pmatrix}\right]_i Y\frac{T_b^2}{2\pi}\sin\beta_i\end{aligned}$$

and hence,

$$\int_0^{T_b}(T_b-t)\vec{y}^b(t)\,dt \approx -Y\frac{T_b^2}{2\pi}\vec{w}. \tag{51}$$

Finally, using the notation

$$\mu=\int_0^{T_b}(T_b-s)\lambda(s)\,ds,$$

the problem to be solved reduces to the following:

Problem 9. *Given periodic currents along the coil sides $I_i(t)$, $i=n_{\rm b}+1,\dots,n_{\rm c}$, find $Y\in\mathbb{R}$, $\beta_1\in[0,2\pi)$ and $\mu\in\mathbb{R}$ such that,*

$$-T_b\mathcal{R}^b\vec{\mathcal{F}}\,(0,Y\vec{u})-\frac{T_b^2}{2\pi}Y\left(\mathcal{R}^b+(\mathcal{A}^b)^\top\mathcal{B}^{-1}\mathcal{A}^b\right)\vec{w}+\mu(\mathcal{A}^b)^\top\begin{pmatrix}\vec{0}\\ \vec{e}\end{pmatrix}=\vec{0}.$$

We notice that β_1 appears in the previous system through $\vec{u}$ and $\vec{w}$. Similarly, $\vec{\mathcal{F}}\,(0,Y\vec{u})$ is defined in terms of $I_i(0)$, $i=n_{\rm b}+1,\dots,n_{\rm c}$, through the solution of Problem 2.

Moreover, in the above system, it is possible to eliminate unknown μ in terms of Y and β_1 (through $\vec{u}$), which is more convenient from the computational point of view. Indeed, taking into account Lemma 8, it is easy to see that

$$-Y\frac{T_b^2}{2\pi}\vec{w}\cdot(\mathcal{A}^b)^\top\begin{pmatrix}\vec{0}\\ \vec{e}\end{pmatrix}=0$$

and, consequently,

$$\mu=\frac{\left(\mathcal{R}^b+(\mathcal{A}^b)^\top\ \mathcal{B}^{-1}\ \mathcal{A}^b\right)^{-1}T_b\mathcal{R}^b\vec{\mathcal{F}}(0,Y\vec{u})\cdot(\mathcal{A}^b)^\top\begin{pmatrix}\vec{0}\\ \vec{e}\end{pmatrix}}{\left(\mathcal{R}^b+(\mathcal{A}^b)^\top\ \mathcal{B}^{-1}\ \mathcal{A}^b\right)^{-1}(\mathcal{A}^b)^\top\begin{pmatrix}\vec{0}\\ \vec{e}\end{pmatrix}\cdot(\mathcal{A}^b)^\top\begin{pmatrix}\vec{0}\\ \vec{e}\end{pmatrix}}.$$

By replacing this expression for μ we get

$$\begin{aligned}\frac{1}{a}\left[\left(\mathcal{R}^b+(\mathcal{A}^b)^\top\ \mathcal{B}^{-1}\ \mathcal{A}^b\right)^{-1}T_b\mathcal{R}^b\vec{\mathcal{F}}(0,Y\vec{u})\cdot(\mathcal{A}^b)^\top\begin{pmatrix}\vec{0}\\ \vec{e}\end{pmatrix}\right](\mathcal{A}^b)^\top\begin{pmatrix}\vec{0}\\ \vec{e}\end{pmatrix}\\ -T_b\mathcal{R}^b\vec{\mathcal{F}}(0,Y\vec{u})-Y\frac{T_b^2}{2\pi}\left(\mathcal{R}^b+(\mathcal{A}^b)^\top\mathcal{B}^{-1}\mathcal{A}^b\right)\vec{w}=\vec{0},\end{aligned} \tag{52}$$

where

$$a:=\left(\mathcal{R}^b+(\mathcal{A}^b)^\top\ \mathcal{B}^{-1}\ \mathcal{A}^b\right)^{-1}(\mathcal{A}^b)^\top\begin{pmatrix}\vec{0}\\ \vec{e}\end{pmatrix}\cdot(\mathcal{A}^b)^\top\begin{pmatrix}\vec{0}\\ \vec{e}\end{pmatrix}.$$

Therefore, Problem 9 can also be written as

Problem 10. *Given periodic currents along the coil sides $I_i(t)$, $i=n_{\rm b}+1,\dots,n_{\rm c}$, find $Y\in\mathbb{R}$ and $\beta_1\in[0,2\pi)$ such that,*

$$\begin{aligned}T_b\left[\frac{1}{a}(\mathcal{A}^b)^\top\begin{pmatrix}\vec{0}\\ \vec{e}\end{pmatrix}\otimes\left(\left(\mathcal{R}^b+(\mathcal{A}^b)^\top\ \mathcal{B}^{-1}\ \mathcal{A}^b\right)^{-\top}(\mathcal{A}^b)^\top\begin{pmatrix}\vec{0}\\ \vec{e}\end{pmatrix}\right)\right]\mathcal{R}^b\vec{\mathcal{F}}(0,Y\vec{u})\\ -T_b\mathcal{R}^b\vec{\mathcal{F}}(0,Y\vec{u})-Y\frac{T_b^2}{2\pi}(\mathcal{R}^b+(\mathcal{A}^b)^\top\mathcal{B}^{-1}\mathcal{A}^b)\vec{w}=\vec{0}.\end{aligned} \tag{53}$$

This is an overdetermined system that can be solved, for instance, in the least-square sense. With this aim, let us define the mapping

$$\vec{f}(Y,\beta_1) := -Y\frac{T_b^2}{2\pi}(\mathcal{R}^b + (\mathcal{A}^b)^\top \mathcal{B}^{-1}\mathcal{A}^b)\vec{w}$$
$$+ T_b\left[\frac{1}{a}(\mathcal{A}^b)^\top \begin{pmatrix} \vec{0} \\ \vec{e} \end{pmatrix} \otimes \left(\left(\mathcal{R}^b + (\mathcal{A}^b)^\top\ \mathcal{B}^{-1}\ \mathcal{A}^b\right)^{-\top} (\mathcal{A}^b)^\top \begin{pmatrix} \vec{0} \\ \vec{e} \end{pmatrix}\right)\right] \mathcal{R}^b\vec{\mathcal{F}}(0, Y\vec{u})$$
$$- T_b\mathcal{R}^b\vec{\mathcal{F}}(0, Y\vec{u}). \quad (54)$$

Then,

$$(Y,\beta_1) = \arg\min_{Z,\,\xi}\left\{ \left\|\vec{f}(Z,\xi)\right\|_2^2 :\ Y_{min} \le Z \le Y_{max},\ 0 \le \xi < 2\pi \right\}.$$

This minimization can be performed with different algorithms, for which, in general, the Jacobian matrix of function $\vec{f}$ with respect to (Y,β_1) should be computed. This can be done from (53) by using the chain rule. Let us introduce the matrix

$$\mathcal{C} := \left[\frac{1}{a}(\mathcal{A}^b)^\top \begin{pmatrix} \vec{0} \\ \vec{e} \end{pmatrix} \otimes \left(\left(\mathcal{R}^b + (\mathcal{A}^b)^\top\ \mathcal{B}^{-1}\ \mathcal{A}^b\right)^{-\top} (\mathcal{A}^b)^\top \begin{pmatrix} \vec{0} \\ \vec{e} \end{pmatrix}\right) - \mathcal{I}\right] \mathcal{R}^b,$$

where $\mathcal{I}$ is the identity matrix. We denote by $\mathrm{D}_{\vec{w}}\vec{\mathcal{F}}(0,\vec{x})$ the Jacobian matrix of mapping $\vec{\mathcal{F}}$ with respect to $\vec{w}$ at point $(0,\vec{x})$. By using (49) we get

$$\frac{\partial\vec{f}}{\partial Y}(Y,\beta_1) = T_b\,\mathcal{C}\,\mathrm{D}_{\vec{w}}\vec{\mathcal{F}}(0,Y\vec{u})\vec{u} - \frac{T_b^2}{2\pi}\left(\mathcal{R}^b + (\mathcal{A}^b)^\top\mathcal{B}^{-1}\mathcal{A}^b\right)\vec{v},$$

$$\frac{\partial\vec{f}}{\partial\beta_1}(Y,\beta_1) = -T_b\,Y\,\mathcal{C}\,\mathrm{D}_{\vec{w}}\vec{\mathcal{F}}(0,Y\vec{u})\vec{v} - Y\frac{T_b^2}{2\pi}\left(\mathcal{R}^b + (\mathcal{A}^b)^\top\mathcal{B}^{-1}\mathcal{A}^b\right)\vec{u}.$$

Let us notice that the calculation of the Jacobian matrix of mapping $\vec{\mathcal{F}}(0,\cdot)$ involves the solution of the magnetostatic problem (23)–(27) for time $t = 0$. We refer the reader to [11] for further details on the computation of this matrix in a similar case.

5. Numerical Results

In this section we present the numerical results obtained for a particular induction machine with squirrel cage rotor, which allow us to validate the methodology proposed in this paper. Therefore, we first use the numerical method proposed in Section 4 to estimate suitable initial currents in the bars of the induction motor. Next, we solve a transient eddy current model using the obtained currents as initial condition and, finally, we compare the time needed to reach the steady-state with the one needed by taking null initial currents. In what follows, we describe some of the characteristics of the machine, which have been provided to us by the company Robert Bosch GmbH. Then, we apply the method to different operating conditions.

5.1. Description of the Machine

A cross-section of the induction machine is sketched in Figure 6. It is composed by $n_\mathrm{b} = 36$ slots in the rotor and 48 slots in the stator.

This induction motor is a three-phase machine having 2 pole pairs with 12 slots per pole. Figure 6 also shows the winding distribution in the stator: red, yellow and blue slots correspond to phases A, B and C, respectively. These source currents are characterized by an electrical frequency f_c and a RMS current I_c

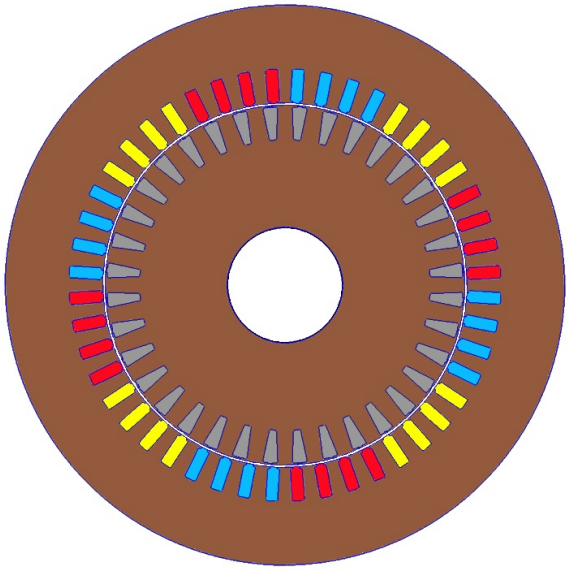

Figure 6: Computational domain. Courtesy of Robert Bosch GmbH.

through each slot. Hence, the analytical expressions of currents corresponding to each phase of the stator are

$$
\begin{aligned}
I_A(t) &= \sqrt{2}\, I_c \cos\left(2\pi f_c t\right), \\
I_B(t) &= \sqrt{2}\, I_c \cos\left(2\pi f_c t + 2\pi/3\right), \\
I_C(t) &= \sqrt{2}\, I_c \cos\left(2\pi f_c t - 2\pi/3\right).
\end{aligned}
$$

Finally, concerning the materials, the rings of the squirrel cage are characterized by a resistance R and the stator coil sides are made of copper. Moreover, the laminated nonlinear material is the electrical steel M330_35A (see [22]).

5.2. Initial Currents for Different Operating Points

We recall that if the currents along the rotor bars are approximated by harmonic functions of frequency f_b, the only unknowns to be determined for computing their initial values are Y and β_1. In particular, we have interpreted β_1 as the phase shift between the current through the first bar and the current corresponding to phase A. In the example, the first bar has been chosen as the one placed in the first quadrant nearest to the horizontal axis. We have approximated these values by

$$
(Y, \beta_1) = \underset{Z,\,\xi}{\arg\min} \left\{ \left\| \vec{f}(Z, \xi) \right\|_2^2 \,:\, Y_{min} \leq Z \leq Y_{max},\ 0 \leq \xi < 2\pi \right\},
$$

where function $\vec{f}$ is defined by (54). In order to validate this methodology, we have considered two operating points corresponding to different electrical sources in the stator and rotational speed n_r; see Table 1. In particular, we notice that the period of the current in the rotor bars, $T_b = 1/f_b$, is one order of magnitude smaller in the second operating point 2 with respect to the first one. However, as we have already mentioned, the methodology to compute the initial currents is time-independent, and therefore its computational cost does not depend on these sizes.

We recall that for a given operating speed n_r and electrical frequency f_c in the stator, T_b can be easily computed as $T_b = 1/s/f_c$ where the slip s is given by $s = (n_s - n_r)/n_s$ and the value of the synchronous speed n_s is computed from the number of poles p (2 in this case) using the relation $n_s = (60 f_c)/p$.

Table 1: Characteristics of the different operating points.

	f_c (Hz)	n_r (rpm)	I_c (A_{RMS})	f_b (Hz)	T_b (s)
Op. Point 1	171.2	5000	314	4.533	0.221
Op. Point 2	632.0	18000	531	531	0.031

For each operating point, we have found the minimum value of function $\|\vec{f}(Y,\beta_1)\|_2^2$ by using the Matlab function `lsqnonlin`. Table 2 shows the optimal values obtained for Y and β_1 and the residual at each operating point. Moreover, in order to measure the computational effort of the `lsqnonlin` function, we have included the initial values ($Y^{(0)}$ and $\beta_1^{(0)}$) the number of nonlinear magnetostatic solutions (NL solutions) and the number of the iterations needed by the `lsqnonlin` function (LSQ iterations). Since the `lsqnonlin` function employs a local search minimization algorithm, to select the global minimum we have provided some starting points in order to choose a local minimum with a minor residual. To perform this task, we have used a multi-start strategy with an average of 25 initial points (5 values for the amplitude Y and 5 values for the phase β_1) for each operating point.

Table 2: Optimal values for the different operating points and computational effort.

	Op. Point 1	Op. Point 2
Y (A)	477.78	942.20
β_1 (rad)	3.34	2.87
$\|\vec{f}(Y,\beta_1)\|^2$	1.12e−08	3.80e−10
$Y^{(0)}$ (A)	400.00	1000.00
$\beta_1^{(0)}$ (rad)	2.00	2.00
LSQ iterations	5	4
NL solutions	6	5

Next, we will analyze the consequence of using these optimal values to define the initial currents along the bars in the transient magnetic simulation.

5.2.1. Sensitivity Analysis of Steady-State in terms of Initial Currents

In this section, we will show that the time needed to reach the steady-state in a transient simulation strongly depends on the choice of the initial currents in the rotor bars of the machine. To attain this goal, we will perform a transient simulation starting with initial currents defined from the values of Y and β_1 found in the previous section. Then, we will compare the results with those corresponding to null initial currents. The initial current intensities for both operating points are shown in Table 3. Due to the machine periodicity, we only specify the values for bars 1 to 9.

To analyze if the solution of the transient eddy current model has reached the steady-state, it is usual to study the torque in the rotor and the currents in the bars of the squirrel cage. We notice that the torque is one of the basic specifications of a motor. In particular, the power output is expressed as its torque multiplied by the rotational speed of the shaft. Figures 7 and 8 show the electromagnetic torque in rotor (left) and the current through the first bar (right) versus time for the two operating points. In these figures, $\tau : \mathbb{R}^+ \longrightarrow \mathbb{R}$ denotes the scalar function that expresses the electromagnetic torque as a function of time. The red curve corresponds to null initial values for the current along the bars, while the blue ones have been obtained by using the values provided by the proposed methodology.

Remark 11. *We emphasize that one of the hypotheses of the procedure for computing suitable initial currents in the rotor bars consists in assuming that these currents are uniformly distributed, i.e., that the rotor bars are stranded conductors. This assumption has allowed us to write an electromagnetic model for the induction machine having time derivatives only in the equation linking currents and voltage drops avoiding,*

Table 3: Initial currents (in A) defined from Y and β_1 for the different operating points.

	Op. Point 1	Op. Point 2
Bar 1	−468.41	−907.66
Bar 2	−407.95	−939.37
Bar 3	−298.29	−857.78
Bar 4	−152.65	−672.73
Bar 5	11.40	−406.53
Bar 6	174.08	−91.31
Bar 7	315.76	234.94
Bar 8	419.35	532.84
Bar 9	472.37	766.48

in particular, the need of solving a parabolic partial differential equation in the bars. However, we emphasize that the transient simulations presented in this section have been performed by considering the bars as solid conductors (see Figure 9), and therefore solving a classical eddy current model coupled with circuit equations, like the one presented, for instance, in [3].

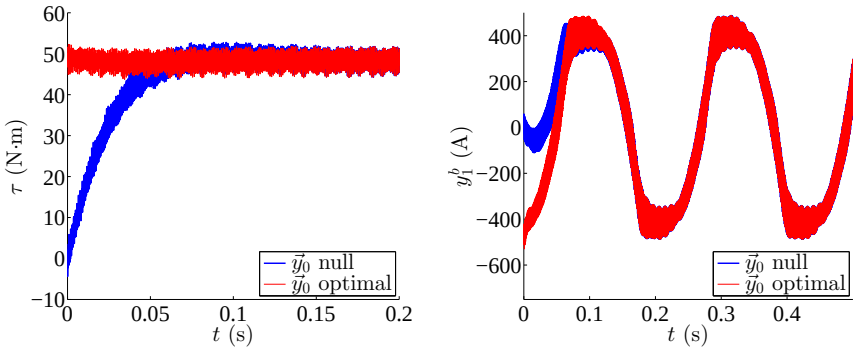

Figure 7: Op. Point 1. Torque vs. time (left). Current in bar 1 vs. time (right).

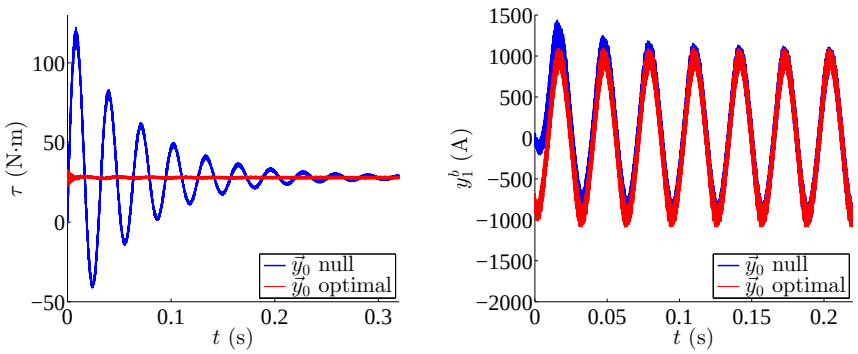

Figure 8: Op. Point 2. Torque vs. time (left). Current in bar 1 vs. time (right).

In order to assess the potential computational saving of the method, we will introduce in the next section a mathematical criterion to achieve the steady-state, what allows us to specify the number of time steps

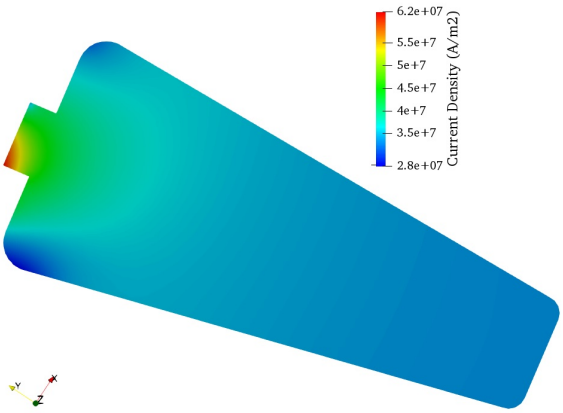

Figure 9: Current density distribution in a rotor bar.

needed to reach such state.

5.2.2. Analysis of the Computational Savings

Let us introduce T_{steady} as the time of the transient FEM simulation for which the steady-state is reached. To define this value, let us denote T_r the mechanical period of the rotor motion, that is, $T_r = 60/n_r$.

For each revolution of the machine, $D_i := [iT_r, (i+1)T_r]$, $i = 0, 1, 2, \ldots$, let us consider its uniform time discretization with time step Δt, which is given by:

$$\{iT_r + j\Delta t, j = 1, \ldots, N\} \subset D_i.$$

Then, the mean torque can be defined as:

$$\tau_i := \frac{1}{N} \sum_{j=1}^{N} \tau \left(iT_r + j\Delta t\right).$$

Thus, T_{steady} will be defined as $T_{\text{steady}} = (m+1)T_r$, with m the first natural number for which the relative error between the mean torque in the m-th revolution and the five subsequent ones is less than 2%. In other words, m is the first natural number for which the following property holds:

$$\frac{|\tau_m - \tau_{m+j}|}{|\tau_m|} < 2\%, \quad j = 1, \ldots, 5.$$

The above criterion has been employed to compute the time to the steady-state for the different operating points under study, with the two different initial conditions. The results have been summarized in Table 4, both in terms of T_{steady} and the number of revolutions needed to achieve convergence.

Figures 10 to 12 show the torque versus time for the considered operating points. In all cases, the time needed to reach the steady-state has been indicated with vertical lines; in particular, in Figure 12, the blue line corresponds to initial condition $\vec{y}^b(0) = \vec{0}$ and the red one to initial condition $\vec{y}^b(0) = Y\vec{u}$. We remark that, in comparison with the case of null initial currents, starting with the initial currents computed with the proposed methodology leads to a very important computational saving.

6. Conclusions

This paper proposes a numerical method to accelerate the computation of the steady-state solution for induction motors with squirrel cage rotor when the periodic currents in the stator coil sides are given. When

Table 4: Time to reach the steady-state for different operating points.

	Initial condition	T_{steady} (s)	Number of revolutions m	Saving (%)
Op. Point 1	$\vec{y}^b(0) = \vec{0}$	0.0840	7	86
	$\vec{y}^b(0) = Y\vec{u}$	0.0120	1	
Op. Point 2	$\vec{y}^b(0) = \vec{0}$	0.3467	104	96
	$\vec{y}^b(0) = Y\vec{u}$	0.0133	4	

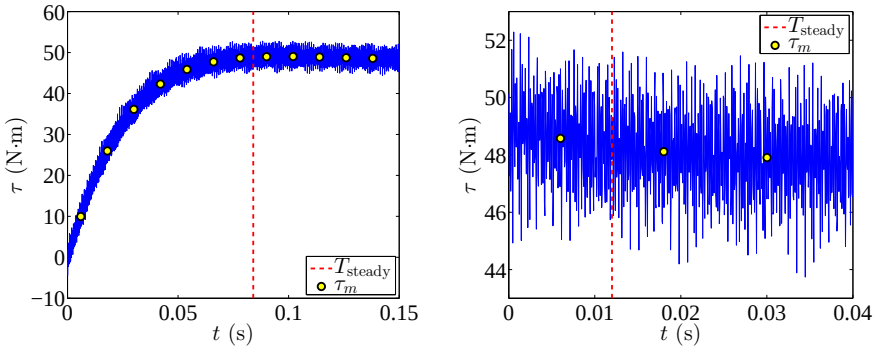

Figure 10: Op. Point 1. Torque vs. time. $\vec{y}^b(0) = \vec{0}$ (left) and $\vec{y}^b(0) = Y\vec{u}$ (right).

a 2D transient magnetic nonlinear model defined in a cross-section of the machine is coupled with circuit equations for the squirrel cage, we obtain a problem in which we also need to provide the initial currents in the rotor bars as data. We focus on approximating these currents in such a way that time-consuming simulations to obtain the steady-state can be shortened. The performance of the methodology is shown with numerical experiments obtained for an induction machine for different operating conditions. In particular, Figures 7 and 8 show that, when starting from the optimal values, the currents reach the steady-state very quickly. On the contrary, the time to reach the steady-state electromagnetic torque can be very large starting from null currents. Moreover, in Table 4 we describe the savings in terms of machine revolutions. These are quite remarkable, specially for the second operating point. It is worth to emphasize that one advantage of our method with respect to others dealing with the same problem is that we only use the periodicity condition in the rotor bars. Thus, limitations appearing in other methodologies related with the presence of several frequencies or the size of the effective period are avoided. Additionally, the problem to be solved to determine the initial conditions is a minimization problem with a very low number of unknowns.

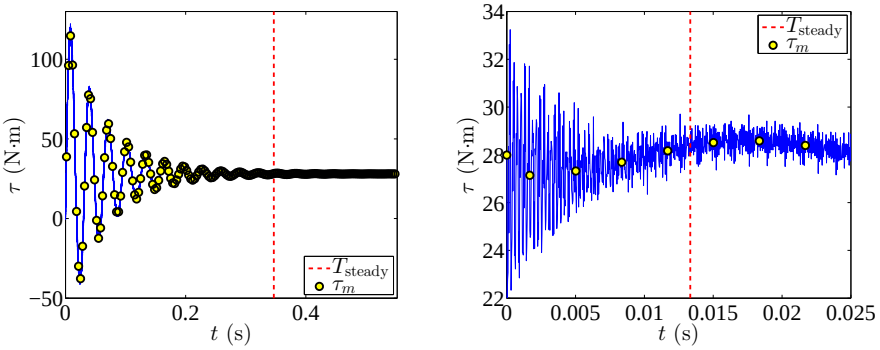

Figure 11: Operating point 2. Torque vs. time. $\vec{y}^{\,b}(0) = \vec{0}$ (left) and $\vec{y}^{\,b}(0) = Y\vec{u}$ (right).

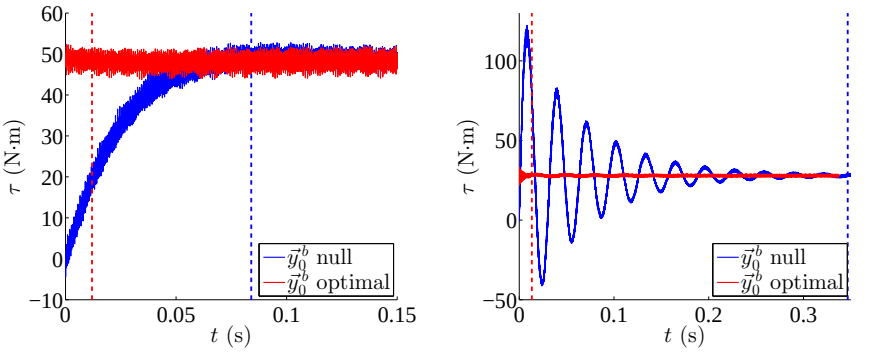

Figure 12: Time to steady-state comparison. Op. Point 1 (left). Op. Point 2 (right).

Acknowledgements

This work has been partially supported by Robert Bosch GmbH under contract ITMATI-C31-2015, by FEDER and Xunta de Galicia (Spain) under grant GI-1563 ED431C 2017/60, by FEDER/Ministerio de Ciencia, Innovación y Universidades-Agencia Estatal de Investigación under the research project MTM2017-86459-R, and by Ministerio de Educación, Cultura y Deporte (Spain) under grant FPU13/03409. The authors express their gratitude to Dr Marcus Alexander and Dr Stefan Kurz from Robert Bosch GmbH for useful discussions about induction machines and for providing us with the data for the numerical experiments.

References

[1] E. Schmidt, Finite element analysis of electrical machines and transformers: State of the art and future trends, COMPEL 30 (6) (2011) 1899–1913.

[2] P. Dular, J. Gyselinck, C. Geuzaine, N. Sadowski, J. P. A. Bastos, A 3-D magnetic vector potential formulation taking eddy currents in lamination stacks into account, IEEE Trans. Magn. 39 (3) (2003) 1424–1427.

[3] V. N. Savov, Z. D. Georgiev, E. S. Bogdanov, Analysis of cage induction motor by means of the finite element method and coupled of field, circuit and motion equations, Electrical Engineering 80 (1997) 21–28.

[4] T. Nakata, N. Takahashi, K. Fujiwara, K. Muramatsu, H. Ohashi, H. L. Zhu, Practical analysis of 3-D dynamic nonlinear magnetic field using time-periodic finite element method, IEEE Trans. Magn. 31 (3) (1995) 1416–1419.

[5] Y. Takahashi, T. Tokumasu, M. Fujita, T. Iwashita, H. Nakashima, S. Wakao, K. Fujiwara, Time-domain parallel finite-element method for fast magnetic field analysis of induction motors, IEEE Trans. Magn. 49 (5) (2013) 2413–2416.

[6] H. Katagiri, Y. Kawase, T. Yamaguchi, T. Tsuji, Y. Shibayama, Improvement of convergence characteristics for steady-state analysis of motors with simplified singularity decomposition-explicit error correction method, IEEE Trans. Magn. 47 (6) (2011) 1786–1789.

[7] K. Miyata, Fast analysis method of time-periodic nonlinear fields, J. Math-for-Ind. 3 (2011) 131–140.

[8] J. Gyselinck, Y. Mollet, R. Sabariego, Steady-state fe modelling of induction machines: the harmonic-balance approach versus the classical fundamental-frequency phasor approach, in: Conférence Européenne sur les Méthodes Numériques en Electromagnétisme (NUMELEC), 2017.
[9] S. Schöps, I. Niyonzima, M. Clemens, Parallel-in-time simulation of eddy current problems using parareal, IEEE Trans. Magn. 54 (3) (2018) 1–4.
[10] A. Stermecki, O. Bíró, K. Preis, S. Rainer, G. Ofner, Numerical analysis of steady-state operation of three-phase induction machines by an approximate frequency domain technique, Elektrotech. Inftech. 128 (3) (2011) 81–85.
[11] A. Bermúdez, O. Domínguez, D. Gómez, P. Salgado, Finite element approximation of nonlinear transient magnetic problems involving periodic potential drop excitations, Comput. Math. Appl. 65 (2013) 1200–1219.
[12] R. Touzani, J. Rappaz, Mathematical Models for Eddy Currents and Magnetostatics with Selected Applications, Springer, 2013.
[13] A. Bossavit, Eddy currents in dimension 2: voltage drops, in: Int. Symp. on Theoret. Electrical Engineering (Proc. ISTET'99, W. Mathis, T. Schindler, eds), University Otto-von-Guericke (Magdeburg, Germany), 1999, pp. 103–107.
[14] S. Kurz, J. Petzer, G. Lehenr, W. Rucker, A novel formulation for 3d eddy current problems with moving bodies using a lagrangian description and bem-fem coupling, IEEE Trans. Magn. 34 (1998) 3068–3073.
[15] A. Buffa, Y. Maday, F. Rapetti, A sliding mesh-mortar method for a two dimensional eddy current model of electric engines, ESAIM: Math. Model. Num. Anal. 35 (2) (2001) 191–228.
[16] F. Bouillault, A. Buffa, Y. Maday, F. Rapetti, Simulation of a magneto-mechanical damping machine: analysis, discretization, results, Comput. Methods in Appl. Mech. Eng. 191 (23–24) (2002) 2587–2610.
[17] A. Bermúdez, D. Gómez, P. Salgado, Mathematical Models and Numerical Simulation in Electromagnetism, New York: Springer, 2014.
[18] A. Bermúdez, M. Piñeiro, P. Salgado, Mathematical and numerical analysis of a transient magnetic model with voltage drop excitations, Comput. Math. Appl. doi:https://doi.org/10.1016/j.camwa.2018.08.054.
[19] B. Heise, Analysis of a fully discrete finite element method for a nonlinear magnetic field problem, SIAM J. Numer. Anal. 31 (3) (1994) 745–759.
[20] N. Deo, Graph Theory with Applications to Engineering and Computer Science, Prentice Hall, 1974.
[21] I. Boldea, S. A. Nasar, The Induction Machine Handbook, CRC Press, 2002.
[22] P. Beckley, Electrical Steels for Rotating Machines, Institution of Electrical Engineers, London, UK, 2002.